



Title	Quantitative Evaluation of Solidification Brittleness of Weld Metal during Solidification by In-Situ Observation and Measurement (Report II) : Solidification Ductility Curves for Steels with the MISO Technique(Materials, Metallurgy & Weldability)
Author(s)	Matsuda, Fukuhisa; Nakagawa, Hiroji; Kohmoto, Hiroaki et al.
Citation	Transactions of JWRI. 1983, 12(1), p. 73-80
Version Type	VoR
URL	https://doi.org/10.18910/7040
rights	
Note	

The University of Osaka Institutional Knowledge Archive : OUKA

<https://ir.library.osaka-u.ac.jp/>

The University of Osaka

Quantitative Evaluation of Solidification Brittleness of Weld Metal during Solidification by In-Situ Observation and Measurement (Report II)†

—Solidification Ductility Curves for Steels with the MISO Technique—

Fukuhisa MATSUDA*, Hiroji NAKAGAWA**, Hiroaki KOHMOTO***, Yoshioki HONDA**** and Yasuhiro MATSUBARA*****

Abstract

Ductility curves of weld metals during weld solidification for tentative plain carbon steels, austenitic stainless steels, and Inconel alloy were constructed by means of the MISO technique and the solidification crack susceptibility of the materials was discussed using minimum ductility required to cause cracking (ϵ_{min}), brittleness temperature range (BTR), and critical strain rate for temperature drop (CST). Influences of carbon, phosphorus and sulphur content on the solidification crack susceptibility were also investigated. It was shown that the values of ϵ_{min} measured by the MISO technique were about one order higher than those measured by ordinary method in all materials. Consequently, ϵ_{min} could be successfully measured even in SUS310S and Inconel 600 which had been difficult to be measured. To evaluate the solidification crack susceptibility of austenitic stainless steels, it would be more proper to use ϵ_{min} which explains the practical tendency much more than BTR or CST. Crack initiation site could be observed in detail and it was revealed that the crack initiation temperature existed very near liquidus temperature except for 0.16% carbon steel.

KEY WORDS: (Solidification) (Hot Cracking) (Carbon Steels) (Stainless Steels) (Welding)

1. Introduction

Solidification cracking during welding has been one of the serious factors that are closely related to the weldability of steels, especially low alloy steels containing relatively higher carbon, nickel or other elements and stainless steels. On the other hand, it is presently considered that the longitudinal cracking in continuous casting could be a solidification cracking. In welding, solidification crack susceptibility of carbon steels except for extremely low carbon steel¹⁾ increases monotonously with an increase in carbon content²⁾. In continuous casting, however, it has been shown³⁾⁻⁸⁾ that the carbon steels containing carbon content of 0.10% to 0.25% is susceptible to the longitudinal cracking. The difference in the effect of carbon content might be revealed by the precise ductility curves of carbon steels with various carbon levels.

General views in regard to the influences of carbon, sulphur, phosphorus and nickel or δ ferrite on suscepti-

bility to solidification cracking has been identically supported in the welding of steels by many researchers. However, to standardize the method to evaluate the susceptibility and to compare it among many kinds of materials, more precise ductility curve is necessary. As shown in the previous paper⁹⁾, the ductility curves constructed by means of the MISO technique which the authors proposed have various merits as compared with those by ordinary methods. In this study, the MISO technique was applied to carbon steels, austenitic stainless steels and Inconel alloy, and the solidification crack susceptibility was discussed on the basis of their ductility curves.

2. Materials Used and Experimental methods

2.1 Materials

Materials used are tentative carbon steels, austenitic stainless steels and Inconel alloy, and their chemical

† Received on April 30, 1983

* Professor

** Research Instructor

*** Graduate Student of Osaka Univ., now with Mitsubishi Metal Corporation

**** Research Associate, Kurume Technical College

Transactions of JWRI is published by Welding Research Institute of Osaka University, Ibaraki, Osaka 567, Japan

Table 1 Chemical composition of materials used

Material	Item	Chemical composition (wt%)								
		C	Si	Mn	P	S	Ni	Cr	Mo	Ti
Plain carbon steel	08C	0.08	0.14	0.28	0.010	0.003	-	-	-	-
	08C-P	0.08	0.14	0.28	0.020	0.003	-	-	-	-
	08C-S	0.08	0.14	0.29	0.010	0.021	-	-	-	-
	16C	0.16	0.14	0.28	0.010	0.004	-	-	-	-
	16C-P	0.16	0.14	0.28	0.020	0.004	-	-	-	-
	16C-S	0.17	0.14	0.29	0.010	0.021	-	-	-	-
	30C	0.31	0.14	0.28	0.010	0.004	-	-	-	-
	30C-P	0.29	0.15	0.29	0.020	0.005	-	-	-	-
	30C-S	0.30	0.14	0.29	0.010	0.021	-	-	-	-
	50C	0.50	0.14	0.29	0.010	0.005	-	-	-	-
Austenitic stainless steel	SUS304L	0.02	0.59	0.99	0.028	0.013	9.75	19.09	0.08	-
	SUS310S	0.07	0.80	1.55	0.016	0.005	20.08	25.00	0.10	-
	SUS316	0.05	0.54	0.81	0.026	0.009	10.48	15.99	1.87	-
	SUS321	0.07	0.96	0.99	0.030	0.007	9.48	18.07	0.14	0.36
Inconel alloy	Inconel 600	0.03	0.13	0.19	0.008	0.001	76.95	16.03	-	-

compositions are shown in **Table 1**. In plain carbon steels, the carbon levels of 0.08, 0.16, 0.30 and 0.50% were selected. In each carbon level, two phosphorus levels of 0.010% and about 0.020% under about 0.003% sulphur and two sulphur levels of about 0.003% and 0.020% under about 0.010% phosphorus were selected respectively. Steels with 0.010% phosphorus and 0.003 to 0.005% sulphur are named "standard materials", and those with about 0.020% phosphorus or 0.020% sulphur are individually named "high phosphorus materials" or "high sulphur materials". Both stainless steels and Inconel alloy 600 are commercial materials.

Shape and size of the specimens used are shown in **Fig. 1**. The thickness of the specimen was 4 mm for carbon steel and 2 mm for stainless steel and Inconel alloy 600.

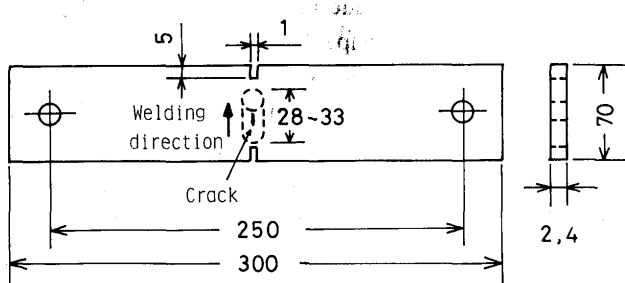


Fig. 1 Shape and size of specimen used for tensile cracking test

2.2 Experimental method

The specimen shown in **Fig. 1** was set to the arrangement of the MISO technique combined with the tensile hot cracking test explained in the previous paper⁹⁾, and rapid strain (132%/sec) was applied perpendicularly to welding direction during welding. The shape of bead is also shown by broken line in **Fig. 1**. Initiation and propagation of solidification cracking are photographed with

high speed cinecamera (about 800 frames/sec) through an optical microscope.

Welding condition, bead width and cooling rate are shown in **Table 2**. The reason why extremely slow welding speed was used is firstly to obtain slow cooling

Table 2 Welding conditions used

Thickness (mm)	Arc voltage (v)	Welding current (A)	Welding speed (mm/min)	Cooling rate behind solidification front (°C/sec)	Bead width (mm)
2	18.5	65	10	10.7	14~15
4	19.5	90	10	12.0	14

rate similar to that in continuous casting and thus to discuss the susceptibility to solidification cracking with relation to the longitudinal crack in continuous casting. The other advantages coming from slow welding are to decrease the moving speed of solidification front and thus to make film analysis of the solidification crackings and their propagations easy. Cinefilm was analyzed by Fixed Gage Method (gage length: 0.9 ~ 1.7 mm)⁹⁾. Details of experimental procedures were mentioned in the previous paper⁹⁾.

3. Experimental Results

3.1 Ductility curves of tentative plain carbon steels

The ductility curves of the standard, high phosphorus and high sulphur materials are shown in **Figs. 2, 3 and 4**, respectively. The T_L in the figures shows the liquidus temperature measured by thermal analysis in electric furnace. Solid marks indicate both the crack initiation temperature (T_C) and the minimum strain or ductility required to cause cracking (ϵ_{min}). The ductility curve constructed by the MISO technique tells the crack initiation temperature clearly, and the characteristic of recovery of ductility from the crack initiation temper-

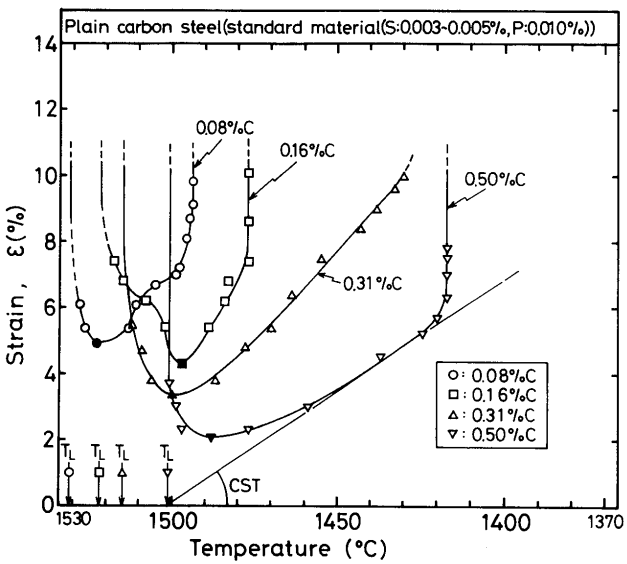


Fig. 2 Ductility curves of standard materials in plain carbon steels

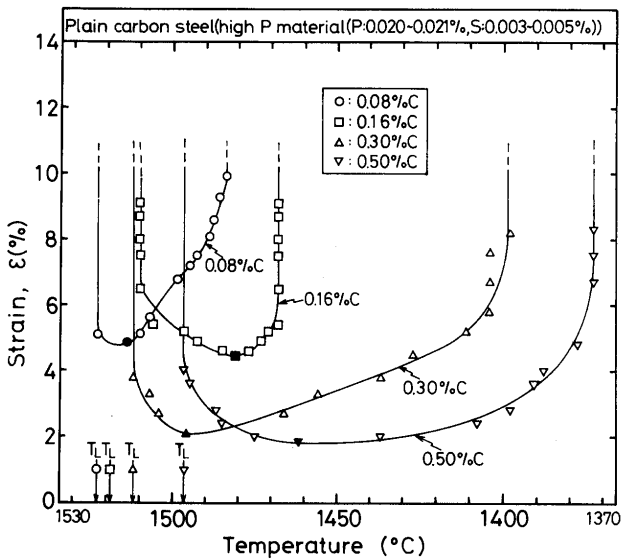


Fig. 3 Ductility curves of high phosphorus materials in plain carbon steels

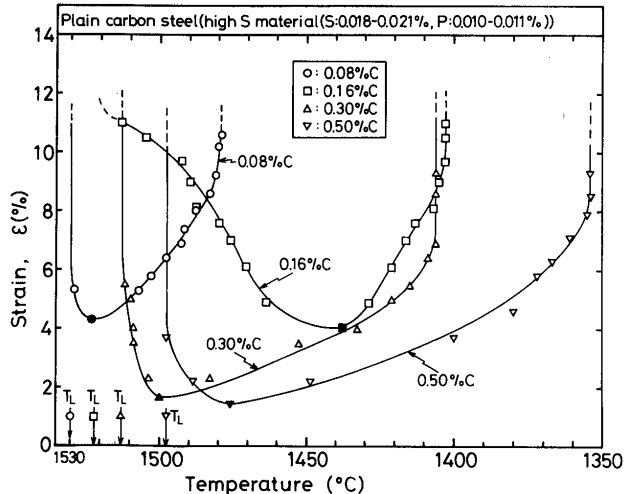


Fig. 4 Ductility curves of high sulphur materials in plain carbon steels

ture toward the higher and the lower temperature regions is well understood.

As mentioned in the previous paper⁹⁾, it is worth noting that ϵ_{\min} values of all materials are considerably high in comparison with those measured by the ordinary Trans-Varestraint Test. For example, while the ϵ_{\min} measured by the Trans-Varestraint Test for SS41 steel (C: 0.22, P: 0.011, S: 0.016%) and S55C steel (C: 0.55, P: 0.014, S: 0.018%) were less than 0.15%¹⁰⁾, the ϵ_{\min} of 16C-P and 16C-S steels which have chemical compositions nearly similar to SS41 and S55C steel were 4.0% and 1.5% in the MISO technique. The new values are about one order higher than the old values. As regards this reason, see ref. 9).

The temperature range enclosed by ductility curve expresses the solidification brittleness temperature range (BTR) which is one of the important factors to estimate the susceptibility to solidification cracking. These figures mean that the enclosed temperature range was nearly saturated at about 10(%) strain, except for the steels 30C and 16C-S. Therefore the enclosed temperature range at about 10(%) strain into which the maximum crack length can be converted was defined as BTR.

3.2 Ductility curves of austenitic stainless steels and Inconel alloy

Figure 5 shows the ductility curves of austenitic stainless steels and Inconel alloy 600. The minimum ductility (ϵ_{\min}) took also considerably higher values in all materials as compared with those measured with the ordinary Trans-Varestraint Test, that is, the value of ϵ_{\min} of SUS321 was 0.4%¹¹⁾ from conventional method and 5.0% from this study. Particularly for SUS310S, it was shown¹⁰⁾ to be impossible to measure the ϵ_{\min} because of

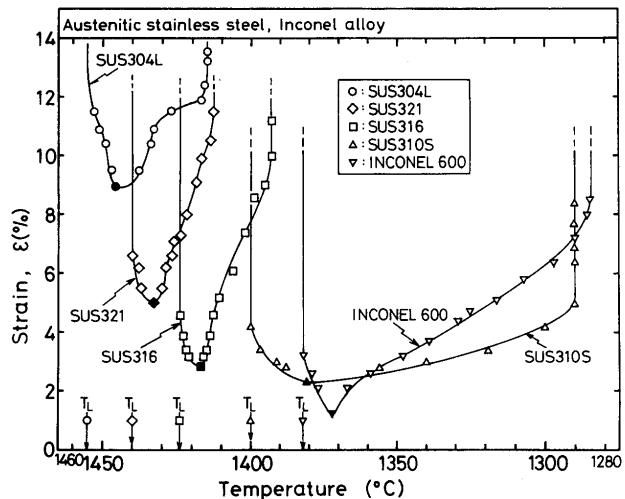


Fig. 5 Ductility curves of different austenitic stainless steels and Inconel alloy

its remarkably small value. In this experiment, however, the ϵ_{\min} could be successfully measured as 2.3% using the MISO technique.

4. Discussion

4.1 Susceptibility to solidification cracking

The relation between carbon content and ϵ_{\min} for the plain carbon steels is shown in Fig. 6. The ϵ_{\min} values of the standard materials decreased linearly with increase in carbon content. In the high phosphorus materials, the

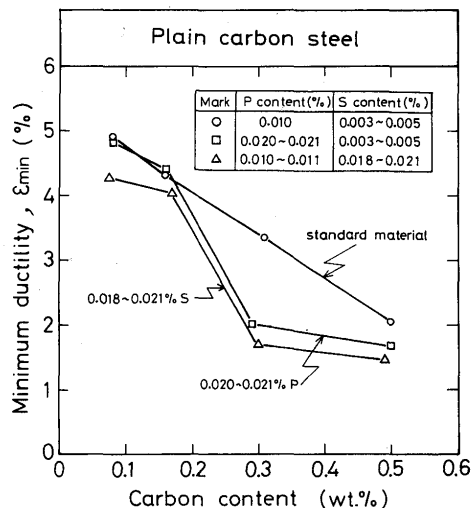


Fig. 6 Minimum ductility (ϵ_{\min}) vs. carbon content in plain carbon steels

ϵ_{\min} values in low carbon levels of 0.08% to 0.16% were approximately the same as those of the standard materials, and phosphorus in the range of carbon content more than 0.30% reduced ϵ_{\min} remarkably. The ϵ_{\min} values of the high sulphur materials were on the whole lower than those of the standard and high phosphorus materials in low carbon levels, and sulphur had the same effect as phosphorus to decrease the ϵ_{\min} values markedly in the range of high carbon content.

It has been generally understood¹²⁾⁻¹³⁾ that in low carbon steels only sulphur influences on the susceptibility to solidification cracking because of low solubility of sulphur in primary δ phase, but in high carbon steels when primary γ phase increases, both sulphur and phosphorus affect the susceptibility. The result of this study well agrees with the tendency.

On the other hand, ϵ_{\min} has been measured concerning the continuous casting of plain carbon steels¹⁴⁾⁻¹⁷⁾, and it is reported¹⁷⁾ that ϵ_{\min} decreases with an increase in solidification temperature range ΔT_{L-S} calculated with an experimental equation¹⁸⁾. The relationship between ΔT_{L-S} and ϵ_{\min} in this study is shown in Fig. 7 in com-

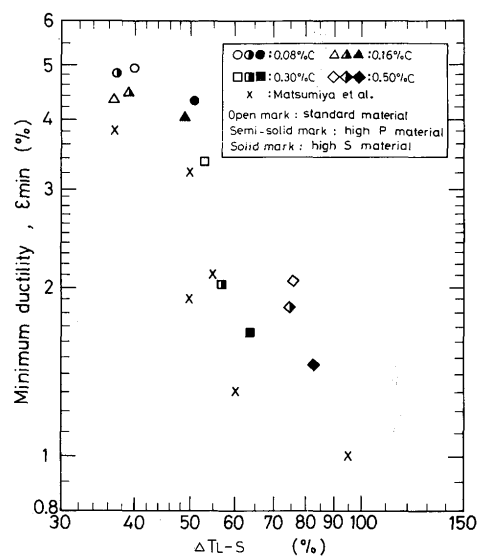


Fig. 7 Minimum ductility (ϵ_{\min}) vs. solidification temperature range (ΔT_{L-S})

parison with the data¹⁷⁾ in continuous casting. The values of ϵ_{\min} obtained from this work were somewhat higher than those measured in continuous casting. The extent of scatter in measured values is within twice for a given ΔT_{L-S} .

The relation between carbon content and BTR is shown in Fig. 8. On the whole, BTR enlarges with an increase in carbon content. In the standard materials, BTR increases greatly while the carbon content rises from 0.16% to 0.30%, and does not change so much from 0.30% to 0.50% carbon. Similar tendency was obtained for the high phosphorus materials. Phosphorus enlarges BTR remarkably in carbon levels from 0.16% to 0.30%,

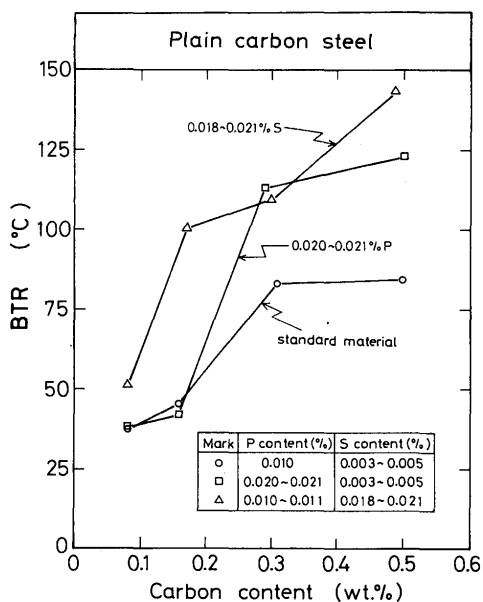


Fig. 8 Brittleness temperature range (BTR) vs. carbon content

though the effect of phosphorus is quite few in the low carbon levels less than 0.16%. The BTR value of the high sulphur materials is wide at every carbon content in comparison with the standard materials, and increases abruptly while the carbon content varies from 0.08% to 0.16%.

It has been generally considered according to Fe-C phase diagram that the width of BTR could depend on ΔT_{L-S} which widens with an increase in carbon content. During solidification, moreover, it is considered that increase in γ phase accompanied with increase in carbon content promote the rejection of phosphorus and sulphur to remaining liquid at interdendritic parts, and then ΔT_{L-S} becomes much wider than as expected from the Fe-C phase diagram. Although manganese is beneficial to suppress the detrimental effect of sulphur as well known, manganese contents of the materials containing carbon content more than 0.16% are too low according to a parameter $[\%Mn]^5/[\%S]^{19, 20}$, and furthermore phosphorus content is too high²¹.

It has been already shown¹⁰) that the shape of ductility curve of a material does not change even if welding conditions are varied. Thus, critical strain rate for temperature drop (CST)¹⁰) was proposed as a good parameter which gives the susceptibility to solidification cracking. As shown in Fig. 2 for 50C steel, CST is defined as the slope of a tangent drawn from the liquidus temperature (T_L) on the abscissa to the ductility curve. CST could be considered to evaluate both ϵ_{min} and BTR collectively. The relationship between carbon content and CST is shown in Fig. 9. The values of CST decrease as carbon content increases. The decreasing rate is steep in carbon

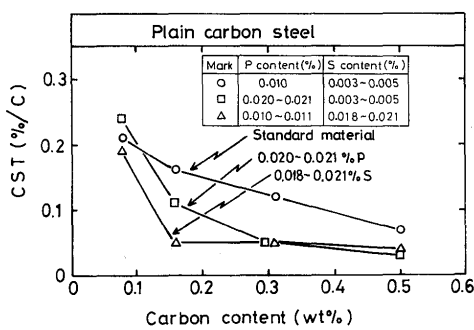


Fig. 9 Critical strain rate for temperature drop (CST) vs. carbon content

level from 0.08% to 0.16% and slow in carbon level more than 0.16%. It could not bring out the result that the CST was lowest at the carbon content near peritectic composition (0.16% C in this work), though steels with about peritectic composition is said to be most susceptible to the longitudinal cracking in the continuous casting³⁾⁻⁸.

The values of ϵ_{min} , BTR and CST for austenitic stainless steels and Inconel alloy are illustrated in Fig. 10. The materials are arranged from left side to right side in the order of low susceptibility to solidification cracking well known in practical welding fabrication except for Inconel 600. Among three parameters expressing the susceptibility to solidification cracking, ϵ_{min} is identical with the order of susceptibility. Beside, ϵ_{min} is measured most easily with the MISO technique. Therefore, ϵ_{min} should be appropriate to estimate the susceptibility to solidification cracking.

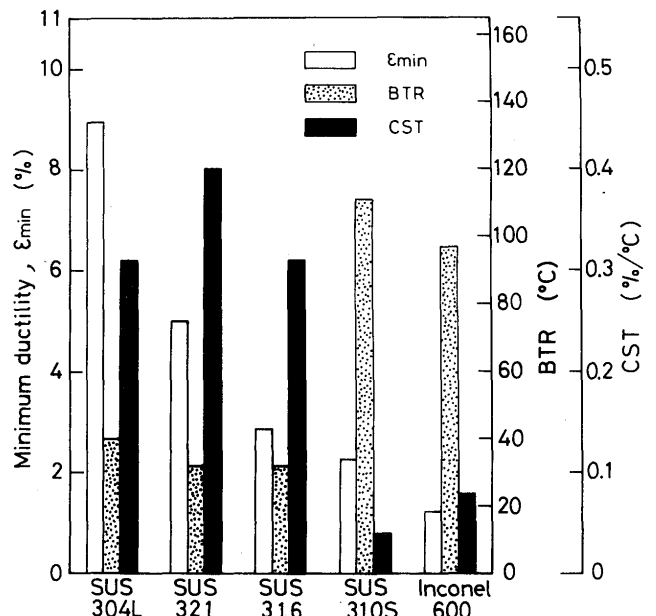


Fig. 10 Illustration of ϵ_{min} , BTR and CST values for each stainless steel and Inconel alloy

4.2 Correlation among each parameter showing solidification crack susceptibility

Mutual relation among ϵ_{min} , BTR and CST from this experiment, namely ϵ_{min} vs. BTR, ϵ_{min} vs. CST and BTR vs. CST are shown in Figs. 11, 12 and 13 respectively. It is seen in Fig. 11 that ϵ_{min} has a tendency to decrease with an increase in BTR. The scatter is, however, large. It may be considered that ϵ_{min} depends on dihedral angle between solid phase and remaining liquid phase, that is, wettability and grain size. On the other hand, BTR is considered to be determined by the actual solidification temperature range²³). Thus ϵ_{min} is independent of BTR in physical sense. For the relation of ϵ_{min} and CST, as shown in Fig. 12, there can not be obvious interrelations, though ϵ_{min} has a rough tendency to increase with an increase in CST. As for the relation between BTR and

CST illustrated in Fig. 13, BTR generally enlarges as CST decreases.

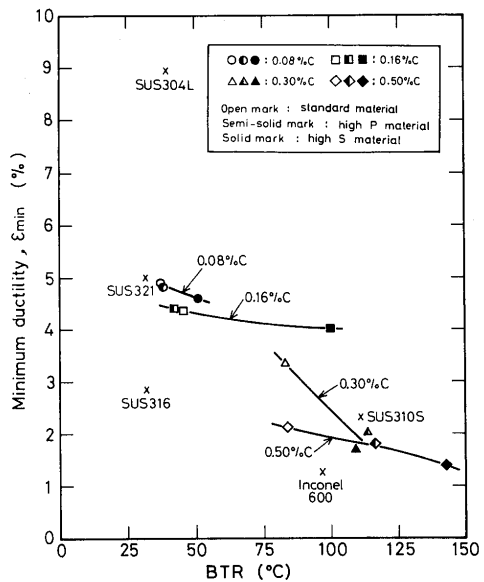


Fig. 11 Minimum ductility (ϵ_{min}) vs. brittleness temperature range (BTR) at $\epsilon = 16\%$

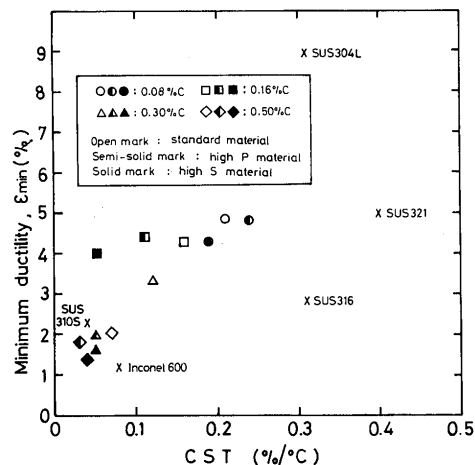


Fig. 12 Minimum ductility (ϵ_{min}) vs. critical strain rate for temperature drop (CST)

4.3 Crack initiation temperature

The relation between carbon content and crack initiation temperature for the plain carbon steels is shown in Fig. 14. The ordinate expresses fractional position of the crack initiation calculated by $\Delta T_{L-C}/BTR \times 100$, where ΔT_{L-C} is the temperature difference between liquidus temperature (T_L) and crack initiation temperature (T_C). The fractional positions of crack initiation in the stainless steels and Inconel alloy are summarized in Table 3. From the figure and the table it is understood that the values of $\Delta T_{L-C}/BTR \times 100$ are about 10 to 20% independently of

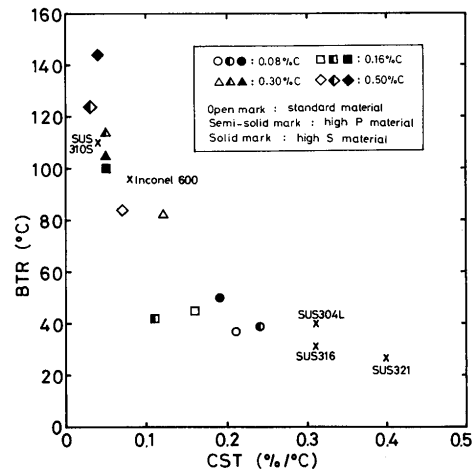


Fig. 13 Brittleness temperature range (BTR) vs. critical strain rate for temperature drop (CST)

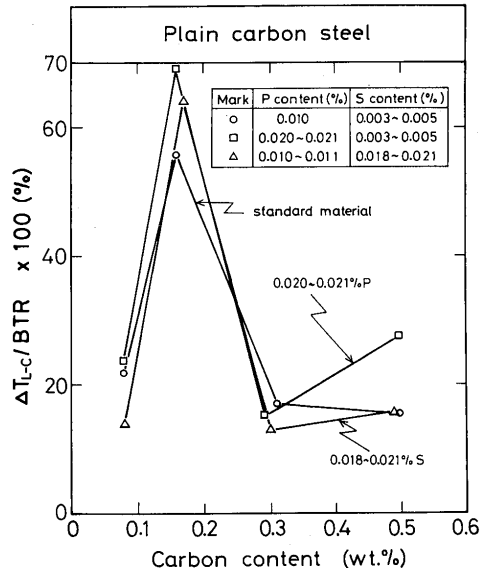


Fig. 14 Fractional position of crack initiation within BTR for carbon steel

Table 3 Fractional positions of crack initiation within BTR for stainless steels and Inconel alloy

Material	$\Delta T_{L-C}/BTR \times 100 (\%)$
SUS304L	20
SUS321	22
SUS316	25
SUS310S	15
Inconel 600	10

carbon contents except for 0.16% carbon steels, which means that crack initiation occurred at considerably higher temperature in BTR. The result that the crack initiation temperature lies near the liquidus differs from

the concept included in Generalized Theory²²). The authors²³ have already given the reason for this.

On the other hand, the values of $\Delta T_{L-C}/BTR \times 100$ only in 0.16% carbon steels, was extremely large, about 60%. In another word, crack initiation occurred in lower temperature region in BTR. Though it is considered that this exceptional result could be related to the peritectic reaction, the reason can not be explained at this moment. In spite of the fact that the longitudinal cracking in continuous casting has often occurred in the steels with similar carbon content, the reason of crack occurrence has not been fully revealed now. Further investigation would be necessary on this problem.

Next, the temperature factors related to the susceptibility to the solidification cracking, that is, liquidus temperature (T_L), crack initiation temperature (T_C) and lower limit temperature of BTR (T_{LBTR}) were illustrated in Fig. 15 for the plain carbon steels in connecting with Fe-C binary diagram. The hatched area shows the solidus temperature calculated from the experimental equation¹⁸. Though T_{LBTR} of the standard materials is in rough agreement with the calculated solidus temperature in all carbon levels. T_{LBTR} of the high phosphorus or sulphur materials with carbon content more than 0.16% lies at 50 ~ 70°C below the calculated solidus temperature.

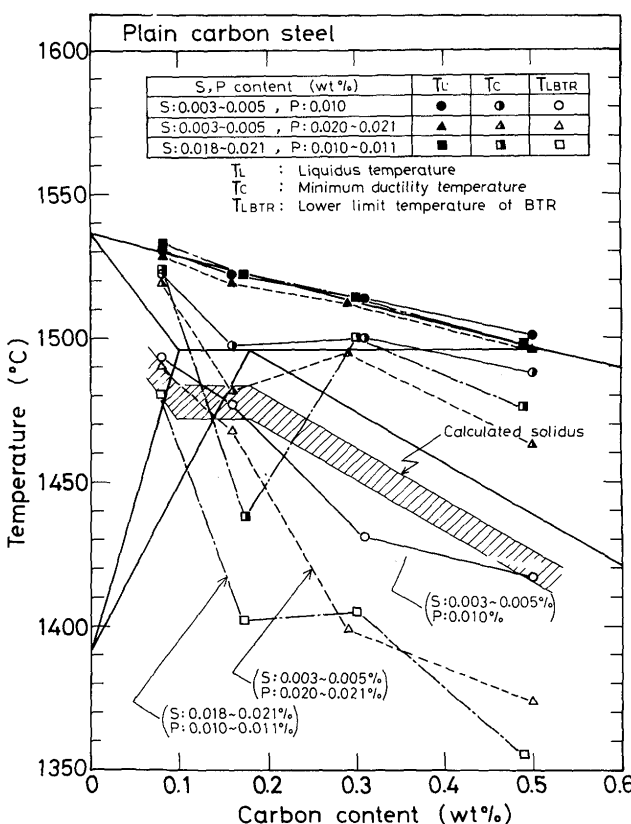


Fig. 15 Illustrations on Fe-C diagram of liquidus temperature (T_L), temperature at ϵ_{min} (T_C) and lower limit temperature of BTR (T_{LBTR}) obtained by experiments

5. Conclusion

Ductility curves of weld metals during weld solidification for tentative plain carbon steels, austenitic stainless steels, and Inconel alloy were constructed by means of the MISO technique, and the solidification crack susceptibility of materials was discussed from minimum ductility required to cause cracking (ϵ_{min}), brittleness temperature range (BTR), and critical strain rate for temperature drop (CST). Influences of carbon, phosphorus and sulphur content on the solidification crack susceptibility were also discussed. Results obtained are:

- 1) The values of ϵ_{min} measured by the MISO technique were about one order higher than those measured with the ordinary Trans-Varestraint Test. The value of ϵ_{min} of SUS310S which has been difficult to be measured because of its too low value with the ordinary Trans-Varestraint Test could be measured easily with MISO technique. From the viewpoint of method for measurement it is considered that the values of ϵ_{min} measured by this method must be correct in comparison with those by the ordinary method.
- 2) The values of ϵ_{min} of the standard plain carbon steel (0.004%S and 0.010%P) decreased linearly as carbon content increased. In the high phosphorus (0.02%P) materials, the values of ϵ_{min} were almost the same values as those of the standard materials in carbon level less than 0.16%, and the ϵ_{min} values were remarkably reduced in carbon level more than 0.30%. In the high sulphur (0.020%S) materials, the value of ϵ_{min} were smaller than that of the standard materials at every carbon level, and sulphur largely reduced ϵ_{min} in the carbon level more than 0.30%. These results well agree with what have been reported for this subject.
- 3) Width of BTR of the standard plain carbon steels increased acutely in the change of carbon content from 0.16% to 0.30%. In the high phosphorus materials, the effect of phosphorus on BTR was not observed in carbon level less than 0.16%, and remarkable in carbon level more than 0.30%. The values of BTR of the high sulphur materials were wholly larger than those of the standard plain carbon steels, and particularly sulphur enlarged BTR acutely in the change of carbon content from 0.16 to 0.30%.
- 4) The value of CST decreased monotonously as carbon content increased.
- 5) Crack initiation generally occurred in high temperature region in BTR except for 0.16% carbon steels where crack initiation occurred in low temperature region in BTR.
- 6) As for the solidification crack susceptibility of austenitic stainless steels, it was found that ϵ_{min} could explain the practical crack tendency much more than BTR or

CST. From above result, it would be more proper to use ϵ_{min} for evaluation of the susceptibility to solidification cracking.

Acknowledgement

The authors would like to thank Committee on Mechanics Behavior of Solidification in Continuous Casting (Chairman Prof. T. Mori) of the Japan Iron & Steel Institute for its supply of materials.

References

- 1) H. Homma, et al: Preprints of National Meeting of Japan Weld. Soc., No. 31 (1982), Autumn, p. 56. (in Japanese)
- 2) J.C. Borland: Brit. Weld. J., Vol. 8 (1961), p. 526.
- 3) R.J. Gray, et al: International Conference on Solidification, 1977 (1979), 300.
- 4) Y. Nuri, et al: J. Iron & Steel Inst. Japan, Vol. 66 (1980), s.807 (in Japanese).
- 5) P. Niles, et al: Steel Making Proceeding, 61 (1978), 399.
- 6) L.I. Morozenskii, et al: Stal. in Eng., 4 (1965), 272.
- 7) T. Saeki, et al: J. Iron & Steel Inst. Japan, Vol. 68 (1982), p. 1773 (in Japanese)
- 8) H. Kitaoka, et al: Committee on Mechanics Behavior of Solidification in Continuous Casting, 1982, Feb. (in Japanese).
- 9) F. Matsuda, et al: Trans. JWRI, Vol. 12 (1983), No. 1, p. 65.
- 10) T. Senda, et al: Trans. Japan Weld. Soc., Vol. 2 (1971), No. 2, p. 1.
- 11) Y. Arata, et al: Trans. JWRI Vol. 6 (1977), No. 1, p. 105.
- 12) F. Matsuda: "Welding Metallurgy", Nikkankogyoshinbunsha, 1972 (in Japanese).
- 13) F. Matsuda: The 65, 66th Nishiyama Memorial Lecture of Iron & Steel Inst. Japan, p. 35 (in Japanese).
- 14) K. Narita, et al: J. Iron & Steel Inst. Japan, Vol. 66 (1980), s806 (in Japanese)
- 15) Y. Sugitani, et al: The 19th Committee of Japan Society for the Promotion of Science (1980) (in Japanese).
- 16) K. Narita, et al: J. Iron & Steel Inst. Japan, Vol. 67 (1981), p. 1307 (in Japanese).
- 17) T. Matsumiya, et al: J. Iron & Steel Inst. Japan, Vol. 69 (1983), s169 (in Japanese).
- 18) M. Hirai, et al: The 19th Committee of Japan Society for the Promotion of Science (1968) (in Japanese).
- 19) H. Nakagawa, et al: Trans. Japan Weld. Soc., Vol. 5 (1974), p. 192.
- 20) H. Nakagawa, et al: Trans. Japan Weld. Soc., Vol. 6 (1975), p. 3.
- 21) H. Nakagawa, et al: Trans. Japan Weld. Soc., Vol. 6 (1975), p. 10.
- 22) J.C. Borland: Brit. Weld. J., Vol. 7 (1960), p. 508.
- 23) F. Matsuda, et al: Trans. JWRI, Vol 11 (1982), No. 2, p. 67.